Journal of Molecular Catalysis A: Chemical 333 (2010) 100–108

Contents lists available at ScienceDirect

Journal of Molecular Catalysis A: Chemical

journal homepage: www.elsevier.com/locate/molcata

Preparation of ceria and titania supported Pt catalysts through liquid phase photo-deposition

S. Scirè[a,*], C. Crisafulli[a], S. Giuffrida[a,**], G. Ventimiglia[b], C. Bongiorno[c], C. Spinella[c]

[a] Dipartimento Scienze Chimiche, Università di Catania, Viale A. Doria 6, 95125 Catania, Italy
[b] Microfluidics Division – Molecular Diagnostics Business Unit, STMicroelectronics, Stradale Primosole 50, 95128 Catania, Italy
[c] CNR-IMM Sezione di Catania, Stradale Primosole 50, 95128 Catania, Italy

ARTICLE INFO

Article history:
Received 4 June 2010
Received in revised form 1 October 2010
Accepted 3 October 2010
Available online 28 October 2010

Keywords:
Catalyst preparation
Liquid phase photo-deposition
Nanoparticles
Ceria
Titania
Deep oxidation
VOC
Structure sensitive reaction

ABSTRACT

The preparation of supported platinum catalysts through a photochemical approach, namely the liquid phase photo-deposition, has been investigated. Pt catalysts were prepared by irradiating at 25 °C and 254 nm an alcohol solution of platinum acetylacetonate complex, where two different supports (ceria or titania) were successively suspended. The prepared catalysts were characterized by TEM analysis and tested for the catalytic deep oxidation of two representative volatile organic compounds, namely toluene and acetone. Results were compared with those from Pt samples prepared by a conventional impregnation technique. It was found that the ceria supported Pt sample prepared by the photochemical approach exhibits much better performance in the combustion of both acetone and toluene, compared to the corresponding impregnated catalyst. A similar trend but to a lesser extent was observed on the Pt/titania series. These results were rationalized on the basis of the different distribution of Pt particles on the support, catalysts prepared by impregnation exhibiting both local massive Pt aggregates and very small Pt particles, samples prepared by photo-deposition showing instead Pt nanoparticles with a homogeneous and narrow size distribution, with diameters in the range of 1.6–2 nm, regarded as appropriate for the deep oxidation of volatile organic compounds.

1. Introduction

The preparation of catalysts is regarded as a fundamental step in the course of the catalytic process playing a key role in the achievement of the desired catalyst performance [1]. Conventional methods for the preparation of supported metal catalysts (impregnation, ion-exchange, co-precipitation, deposition–precipitation) involve two main steps, consisting of the introduction of the metal precursor on the support and the successive transformation of the precursor to the active metallic phase [1]. Due to the high number of variables involved in both steps, it is difficult to get complete control on all parameters and therefore reproducible results are not easily achievable. Moreover, these conventional methods generally lead to metal particles which are often non-uniformly spread on the support surface and with wide particle size distributions. The synthesis of metal particles with a controlled and narrow distribution is instead a critical factor chiefly for those catalytic reactions which are dependent on particle dimensions (the so-called structure-sensitive reactions) [2]. In the last decades chemical vapour deposition (CVD) gained interest in the preparation of supported catalysts being a flexible and reproducible technology. However, CVD presents several disadvantages, such as the requirement of precursors with high vapour pressure, which are often hazardous and extremely toxic, and the necessity to employ high temperatures for precursor decomposition, which can lead to catalyst deactivation [1].

In recent years, alternative routes to the preparation of supported catalysts from liquid phase based on the use of preformed clusters or templating agents have been proposed to obtain more uniform catalysts [3,4], with the specific purpose to control the formation of metal bonds or metal particles in solution and then delivering them to the support surface preserving the metal particles morphology [5]. The application of such an approach remains problematic, however, for instance in the case of Pt, because the removal of ligands or templating agents leads to substantial metal sintering [4,6]. In order to overcome this drawback Siani et al. recently proposed the use of an unprotected stable colloidal Pt suspension for the preparation of Pt/γ-Al_2O_3 catalysts [7].

Recently, we reported the preparation of γ-alumina supported Pt catalysts with a very narrow particle size distribution through a photochemical approach, namely the liquid phase photo-deposition (LPPD) technique, which allows the direct deposition of active metallic species on the support from the liquid phase at

* Corresponding author. Tel.: +39 0957385112; fax: +39 095580138.
** Corresponding author. Tel.: +39 0957385063.
E-mail addresses: sscire@unict.it (S. Scirè), sgiuffri@unict.it (S. Giuffrida).

1381-1169/$ – see front matter © 2010 Elsevier B.V. All rights reserved.
doi:10.1016/j.molcata.2010.10.003

room temperature by means of quite simple and economic equipment [8]. LPPD involves the chromophore of a metal complex which is able to absorb the light producing a photo-excited state which may decompose, by a photo-redox reaction, to give an unprotected solid metallic phase cluster able to spread over the support surface [9,10]. Recently we also reported the preparation of supported Ag catalysts through a modified photochemical approach consisting in the photo-assisted preparation of stable unprotected Ag colloids in water, followed by the deposition of Ag nanoparticles on the support [11].

The goal of this work was to evaluate the role of the support in the preparation of supported Pt catalysts through LPPD. Two different supports, namely ceria and titania, were investigated and the results were compared to those previously reported for alumina supported Pt samples prepared by the same photochemical approach [8].

The $Pt(acac)_2$ complex was chosen as precursor of platinum. The β-diketonates of metals are interesting compounds both from an applicative and theoretical point of view. They have been used as precursors in the metal-organic chemical vapour deposition (MOCVD) to obtain thin films of metals and their oxides, due to their volatility and are also good candidates for photochemical studies in the gas phase, being able to absorb UV and visible light. These features make these compounds suitable for photo-CVD [12], a technique exploiting radiation (in particular UV) as an energy source to obtain deposition of metals and/or oxides using temperatures lower than in thermal MOCVD. Because the β-diketonates are readily soluble in organic solvents they can also be used for liquid phase photo deposition [8].

The catalytic activity of Pt catalysts prepared by LPPD was evaluated for the deep oxidation of two organic compounds, namely toluene and acetone, which were chosen as representatives of volatile organic compounds (VOC). The catalytic behaviour and physical properties of these catalysts (samples coded as PD) were compared with those of Pt samples prepared on the same supports by the conventional wetness impregnation technique, using the most common Pt precursor, namely H_2PtCl_6 (samples coded as IM).

2. Experimental

2.1. Catalyst preparation

The metal oxides used as supports were TiO_2 (Degussa P25, surface area of $50\,m^2\,g^{-1}$, containing anatase and rutile phases in a ratio of about 3:1) and CeO_2 (surface area of $110\,m^2\,g^{-1}$), prepared in laboratory by precipitation with KOH from $Ce(NO_3)_3 \times 6H_2O$ according to the procedure elsewhere reported [13]. The $Pt(acac)_2$ complex (acac = 2,4-pentandionate anion), reagent grade (Aldrich), was used without further purification. Anhydrous ethanol (Carlo Erba) was spectrophotometric grade.

Kinetic experiments were carried out by irradiating the ethanol solution of $Pt(acac)_2$, 5×10^{-4} M, at 25 °C and 254 or 350 nm in a quartz cuvette using a Rayonet Photochemical Reactor (Italquartz) equipped with various numbers of lamps. The light intensity, measured by a ferric oxalate actinometer [14], was 1.0×10^{-6} Nhν min^{-1} (2.7 mW cm^{-2}). The kinetics of the $Pt(acac)_2$ photo-reduction were followed spectrophotometrically at 350 nm (at this wavelength the released Hacac ligand does not absorb).

For the preparation of supported Pt catalysts through LPPD, the ethanol solution of $Pt(acac)_2$, 5×10^{-4} M, was irradiated in a quartz vessel at 25 °C and 254 nm with a light intensity of 1.0×10^{-5} Nhν min^{-1}, until complete platinum photo-reduction. The support (CeO_2 or TiO_2) was added successively to the Pt colloidal solution, leaving under vigorous stirring at room temperature until disappearance of platinum from the solution (this required about 2 h). This was followed spectrophotometrically monitoring, on a clear solution obtained by filtration of a little amount of suspension, the disappearance of the structureless absorption, extending up to visible region, due to the light scattering of Pt nanoparticles. After completion of the deposition of the metal onto the support, the suspended material was recovered by centrifugation and washed several times with pure ethanol and then dried in an oven at 90 °C. Pt samples prepared through the above reported photochemical approach were coded with the suffix – PD.

For comparison Pt catalysts (coded with suffix – IM) were prepared by conventional incipient wetness impregnation of the support with an aqueous solution of H_2PtCl_6 (Alfa Aesar). These samples were dried at 110 °C for 24 h and reduced in flowing H_2 at 350 °C for 1 h, before their further use.

All samples (PD and IM) were prepared in order to have a nominal 1 wt.% Pt loading.

2.2. Colloidal solutions and supported catalysts characterization

Ultraviolet–visible absorption spectra were recorded with a Hewlett–Packard 8452A diode array and a UV-VIS Jasco V-560 spectrophotometer.

Dynamic Light Scattering (DLS) was carried out using a LB-550 HORIBA size analyzer equipped with a Laser diode at 650 nm.

Transmission electron microscopy was performed with a TEM JEOL JEM 2010 F, equipped with the Gatan imaging filter, operating at 200 keV. Samples for TEM were prepared by placing several drops of the colloidal dispersions of catalysts onto a carbon-coated copper micro-grid (2 M STRUMENTI). In order to obtain a good statistical particle size distribution several different areas of the grid were observed and more than 150 Pt particles measured for each sample. The average size diameter estimated by TEM was calculated using the following formula: $d = \sum(n_i d_i)/n$, where n_i is the number of Pt particles of diameter d_i and n is the total number of Pt particles.

H_2 chemisorption was carried out in a pulse reactor system in which fixed volumes of H_2 were introduced at room temperature through an injection valve. Before the measurements samples were reduced in H_2 at 350 °C for 1 h, maintained at this temperature in flowing Ar for 1 h and then cooled at room temperature always in Ar.

2.3. Catalytic activity measurements

Catalytic activity tests were performed in a continuous-flow fixed-bed microreactor in the gas phase at atmospheric pressure, using 0.1 g of catalyst (80–140 mesh) diluted with an inert glass powder. The reactant mixture was fed to the reactor by flowing a part of the He stream through a saturator containing the VOC and then mixing with O_2 and He before reaching the catalyst. The reactant mixture was 0.7 vol.% VOC and 10 vol.% O_2, the remainder being helium. A space velocity (GHSV) of 7.6×10^{-3} mol h^{-1} g_{cat}^{-1} was always used. The effluent gases were analysed on-line by a gas chromatograph (Thermo), equipped with a packed column with 10% FFAP on ChromosorbW and FID detector, and by a quadrupole mass spectrometer (VG quadrupoles). For all experiments CO_2 was the main carbon-containing product, only very small amounts of CO were found at low conversions. The carbon balance was always higher than 95%. Preliminary runs carried out at different flow-rates showed the absence of external diffusional limitations. The absence of internal diffusion limitations was verified by running experiments with catalyst powders at different grain size.

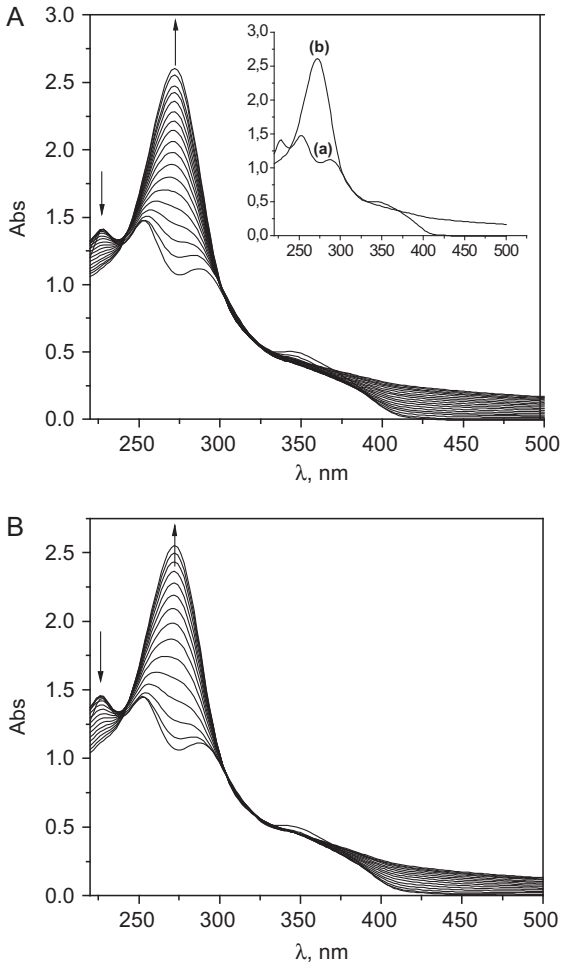

Fig. 1. (A) Spectral changes of ethanol solution 1.5×10^{-4} M in $Pt(acac)_2$, irradiated at 350 nm ($I = 1 \times 10^{-6}$ Nhν min^{-1}, 2.7 mW cm^{-2}) at various times (0–340 min). The spectra were registered every twenty minutes. The quantum yield was, $F = 0.50 \times 10^{-3}$. Inset: initial (a) and final (b) spectrum. (B) Spectral changes of ethanol solution 1.5×10^{-4} M in $Pt(acac)_2$, irradiated at 254 nm ($I = 1 \times 10^{-6}$ Nhν min^{-1}, 2.7 mW cm^{-2}) at various times (0–140 min). The spectra were registered every 10 min. The quantum yield was, $F = 0.52 \times 10^{-3}$.

3. Results

3.1. Kinetics of the Pt complex photodecomposition

The electronic absorption spectrum of a thermally stable solution of $Pt(acac)_2$ in anhydrous ethanol displays (Fig. 1A, inset spectrum (a)) four distinct bands at 225 nm (ε = 11,200), 250 nm (ε = 10,000), 290 nm (ε = 7300) and 345 nm (ε = 3500). Irradiation at any of the four wavelengths resulted in equally efficient reduction of the Pt–β-diketonates complex. In fact the spectral changes of the $Pt(acac)_2$ ethanol solution (1.5×10^{-4} M) show the same trend, when irradiated, with the identical light intensity, both at 350 (Fig. 1A) and 254 (Fig. 1B) nm. The figures show that the disappearance of the $Pt(acac)_2$ absorption bands (225, 250, 290 and 345 nm) was accompanied by the appearance of the typical absorption band of Hacac (λ_{max} = 274 nm), consistent with a π–π^* (HOMO–LUMO) transition [15], and a structureless absorption extending up to the visible region, attributed to the formation of Pt nanoparticles. It is noteworthy that at the end of photochemical reduction, the released ligand concentration, detected by UV spectrophotometer, was double the amount of the starting complex concentration. It must also be underlined that the quantum yield, calculated by the ratio between initial disappearance of the complex and number of absorbed photons by reactive species, is independent upon the wavelength of the light because the photoreduction arises from a single excited state reached by the internal conversion from the excited state populated by direct irradiation at various wavelengths. However, it can be observed that different times were necessary to reach the complete photo-reduction (140 and 340 min for irradiation at 254 and 350 nm respectively). This finding can be explained taking into account the different fraction of light absorbed from the initial complex solution at the two different wavelengths (Fig. 1A, inset spectrum (a)).

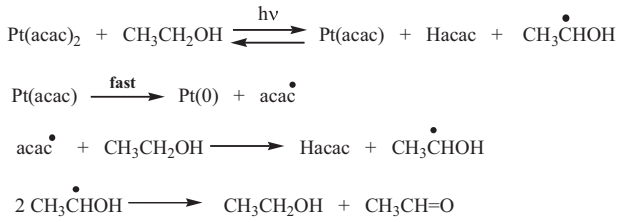

Scheme 1.

The photo-reduction mechanism of the $Pt(acac)_2$ complex in ethanol (Scheme 1) has been previously reported [8] and is believed to involve the cleavage of the Pt–O bond, the formation of a three-coordinated intermediate which gives hydrogen abstraction from the solvent with formation of Hacac and a Pt intermediate which rapidly decomposes to Pt° and acetyl–acetonyl radical. The radical abstracts a hydrogen atom from the solvent giving a molecule of the free ligand, Hacac. The ethanol radical can decay through dismutation to aldehyde and alcohol.

The size of platinum nanoparticles in ethanol solution was determined by Dynamic Light Scattering (DLS) analysis. Fig. 2 displays the particle size distributions of Pt nanoparticles, after irradiation of the ethanol solution of $Pt(acac)_2$ at 254 (curve a) or 350 nm (curve b). The figure points out that irradiation at 254 nm leads to smaller Pt particles compared to irradiation at 350 nm. A mean diameter of 6 nm and 8.5 nm for samples irradiated respectively at 254 and 350 nm was, in fact, observed. This behaviour agrees well with the higher ε value of the $Pt(acac)_2$ solution measured at 254 nm with respect to 350 nm, justifying the higher irradiation time necessary at this latter wavelength to completely reduce the Pt complex. It has been, in fact, reported that the metal nanoparticles dimension depends on the ratio of the nucleation

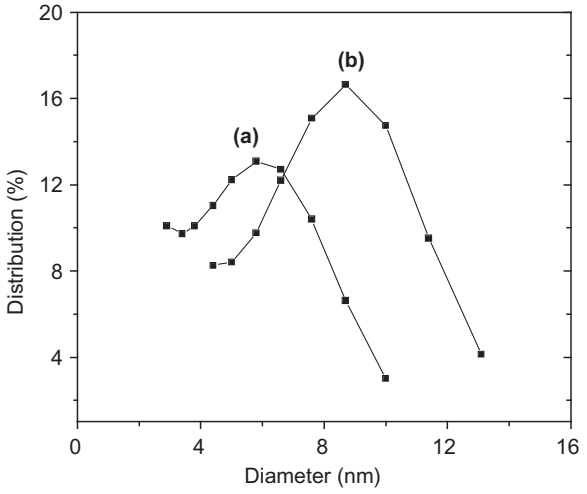

Fig. 2. Particle size distribution obtained by DLS of Pt nanoparticles after irradiation of an ethanol solution of $Pt(acac)_2$ at (a) 254 nm, $t_{irrad.}$ = 130 min and (b) 350 nm, $t_{irrad.}$ = 340 min. $I = 1 \times 10^{-6}$ Nhν min^{-1}.

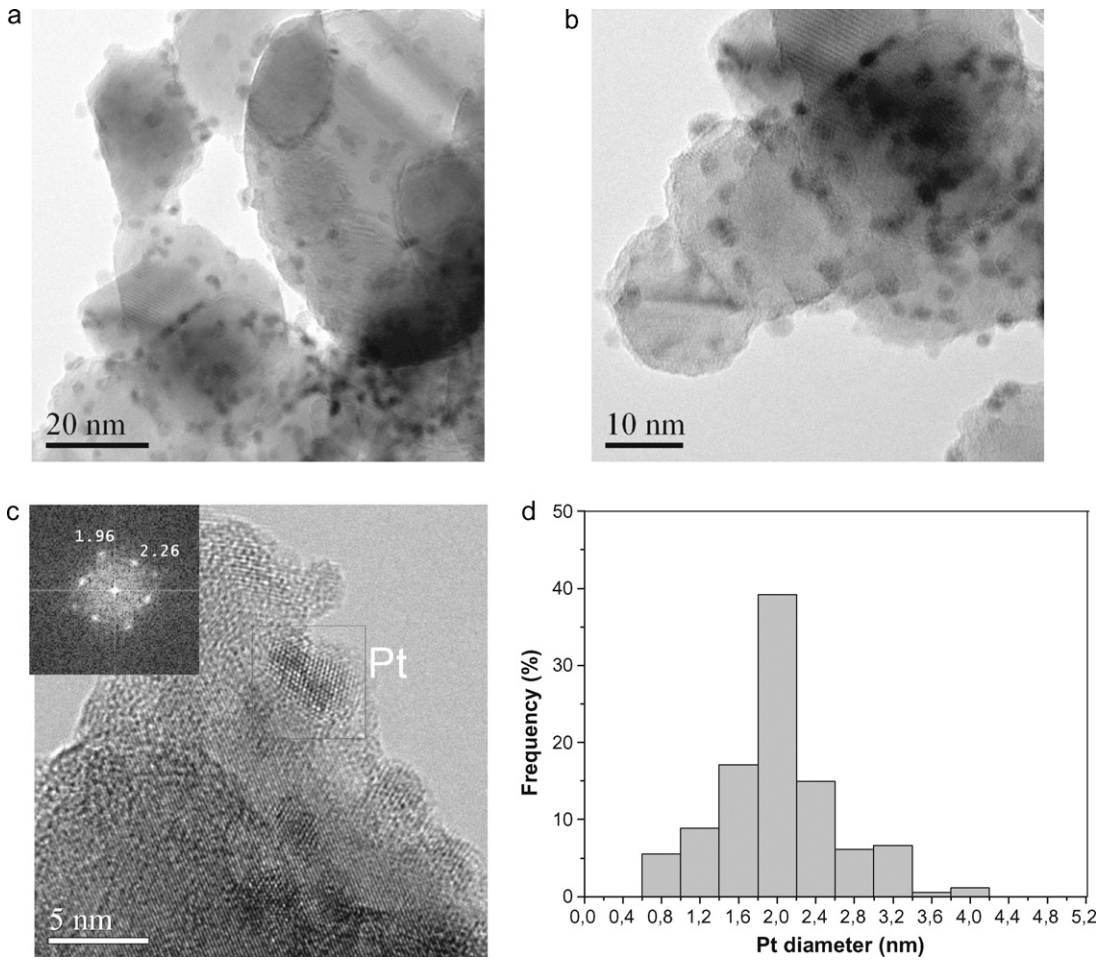

Fig. 3. TEM microphotographs (a–c) and particle size distribution (d) for the Pt/TiO_2-PD sample.

rate to the growing rate of metal particles, a higher ratio leading to smaller particles [16,17]. An analogous effect of the light wavelength on the dimension of metal nanoparticles has been reported in the case of the preparation of Ag colloids in water by Ag(acac) photo-reduction [11].

3.2. Preparation of supported Pt catalysts

On the basis of considerations reported in the previous section, the preparation of supported Pt catalysts by LPPD was carried out at the wavelength of 254 nm and the highest light intensity allowed by the experimental apparatus ($I = 1.0 \times 10^{-5}$ Nhν min^{-1}) with the aim to shorten the irradiation time thus obtaining Pt particles with a smaller size. It is important to note that the time required to have a complete photo-reduction of the Pt complex was strongly dependent on the presence and the nature of the support suspended in the ethanol solution. In fact, the photo-reduction of the Pt complex, under the experimental conditions used ($\lambda = 254$ nm and $I = 1.0 \times 10^{-5}$ Nhν min^{-1}) required around 30 min in the absence of the support, two hours with ceria, whereas in the presence of TiO_2 it was not possible to accomplish a complete photo-reduction in 24 h. This behaviour can be explained on the basis of the different distribution of light between the support and the Pt complex. In fact, as verified by UV experiments, ceria suspensions partially scatter the radiation thus reducing the amount of light reaching the Pt complex, whereas with titania, due to its strong ability to both adsorb and scatter the UV-light employed during irradiation, the amount of radiation available is very low and not sufficient to complete the photo-reduction of the complex in a reasonable time. This also excludes the photocatalytic reduction of the Pt complex by the titania support. Therefore to overcome this drawback and to shorten the irradiation time we decided to prepare both Pt/TiO_2 and Pt/CeO_2 catalysts adding the support to the colloidal solution only after the complete platinum photo-reduction was accomplished, then leaving under vigorous stirring at room temperature until complete disappearance of platinum from the solution (this requires about 2 h).

3.3. TEM characterization of supported Pt catalysts

Transmission electron microscopy was carried out in order to characterize metallic platinum nanoparticles of prepared supported catalysts. Figs. 3–5 report TEM microphotographs of investigated titania supported Pt samples, namely Pt/TiO_2-PD (Fig. 3), Pt/TiO_2-PD treated in H_2 at 350 °C (Fig. 4) and Pt/TiO_2-IM (Fig. 5).

The bright field images reported in Fig. 3a–c show very small and round shaped Pt particles homogeneously spread on the surface of bigger titania grains. Fast Fourier Transformation in the inset of Fig. 3c clearly shows the diffraction pattern of Pt, thus confirming the chemical nature of the dispersed nanoparticles. Particle size analysis (Fig. 3d) shows a very narrow and symmetric distribution of Pt nanoparticles, with an average diameter of 2.0 nm. In the case of the Pt/TiO_2-PD sample treated in H_2 at 350 °C (Fig. 4) both Pt particles and titania grains show the same morphology (Fig. 4a) and very similar size distribution (Fig. 4b) than the untreated Pt/TiO_2-PD sample (Fig. 3). This confirms that the

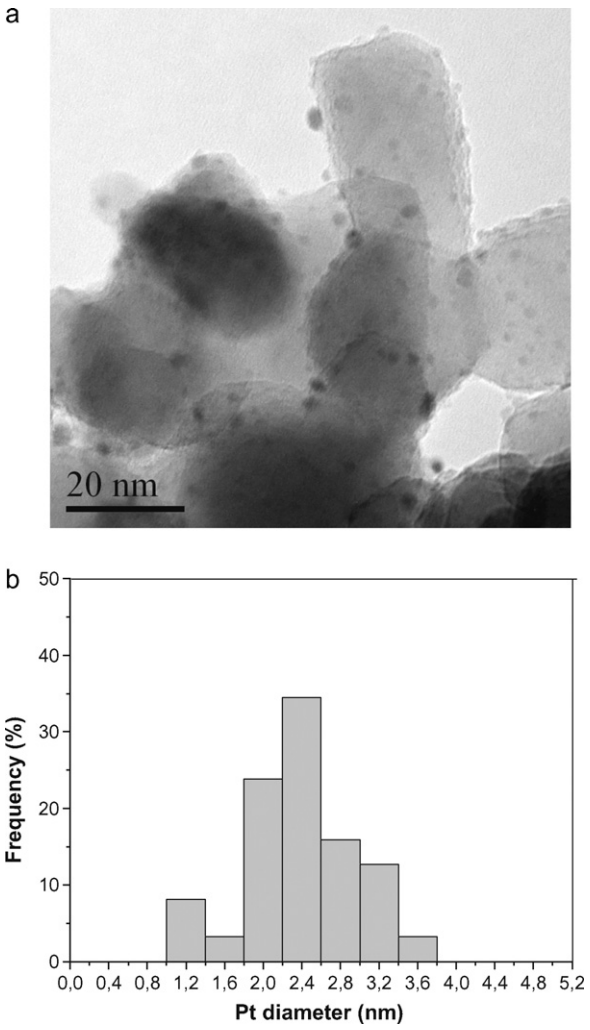

Fig. 4. TEM microphotographs (a) and particle size distribution (b) for the Pt/TiO_2-PD sample after treatment in H_2 at 350 °C.

thermal process with H_2 does not substantially affect the structural features of the catalyst, which were determined by the preparation method. The Pt/TiO_2-IM sample (Fig. 5) shows a significantly different morphology compared to that of the sample prepared by the photochemical approach. It can be noted, in fact, that the Pt/TiO_2-IM sample exhibits clustering of Pt particles resulting in massive aggregates of not well distinguishable units. These aggregates are spread on the titania support, drawing "worm" shapes around the edges of the grains, as evidenced in the magnification of Fig. 5b.

TEM microphotographs of investigated ceria supported Pt samples are reported in Fig. 6 (Pt/CeO_2-PD) and Fig. 7 (Pt/CeO_2-IM). It must be preliminary underlined that the TEM photos of Pt/ceria catalysts were not so well resolved as Pt/titania ones, due to the low contrast between Pt and ceria. Nevertheless, the degree of resolution was enough to find differences between the two catalysts prepared by the different approaches. The sample prepared by the photochemical technique is featured by Pt nanoparticles homogeneously distributed over the entire support surface. Although the low contrast did not allow to perform a satisfactory size distribution, however, on the basis of the evaluation on groups of better resolved particles (Fig. 6b), it can be stated that most particles have diameter in the range 1.6–2 nm. In contrast, on the sample prepared by the standard impregnation method Pt nanoparticles appear not to be homogeneously distributed over the surface, showing both local phenomena of massive Pt aggregation (Fig. 7a) and very small Pt particles, with diameters around or lower than 1 nm (Fig. 7b), which is near the resolution limit of the instrument.

3.4. H_2 chemisorption on supported Pt catalysts

H_2 chemisorption was carried out in order to determine the Pt dispersion and average particle size of investigated catalysts with the aim to compare the results with those obtained by TEM. Obtained chemisorption data have shown that the amount of H_2 chemisorbed on both Pt/TiO_2-IM and Pt/TiO_2-DP samples was considerably low. Assuming a stoichiometry of H/Pt = l/l, dispersions of 6% and 16% were calculated for Pt/TiO_2-IM and Pt/TiO_2-DP respectively. Pt sizes, estimated on the basis of the above dispersions, assuming spherical Pt particles, were 18.8 nm (Pt/TiO_2-IM) and 7.1 nm (Pt/TiO_2-DP), values sensibly higher than those obtained by TEM. According to the literature, this discrepancy can be reasonably explained on the basis of the occurrence of a strong metal-support interaction (SMSI) between Pt and TiO_2, which strongly inhibits the adsorption of H_2 on Pt [18,19]. On the contrary on both Pt/CeO_2-IM and Pt/CeO_2-DP samples the amount of H_2 chemisorbed was very large with H/Pt ratios higher than 5 (5.8 and 5.7 for Pt/CeO_2-IM and Pt/CeO_2-DP, respectively), suggesting that hydrogen spillover takes place between platinum and the support. Hydrogen spillover

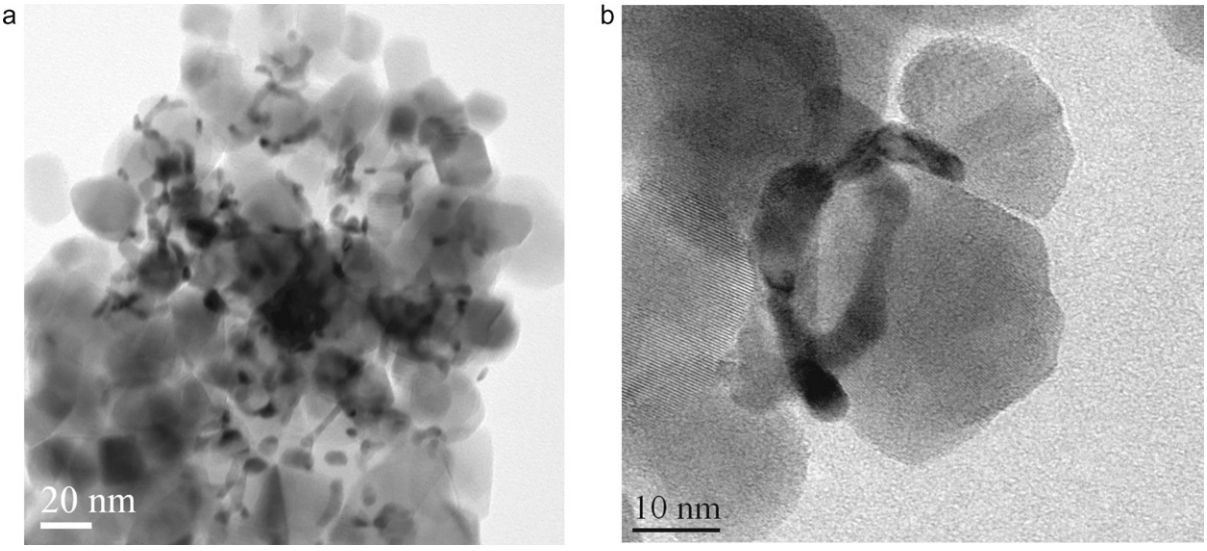

Fig. 5. TEM microphotographs (a and b) for the Pt/TiO_2-IM sample.

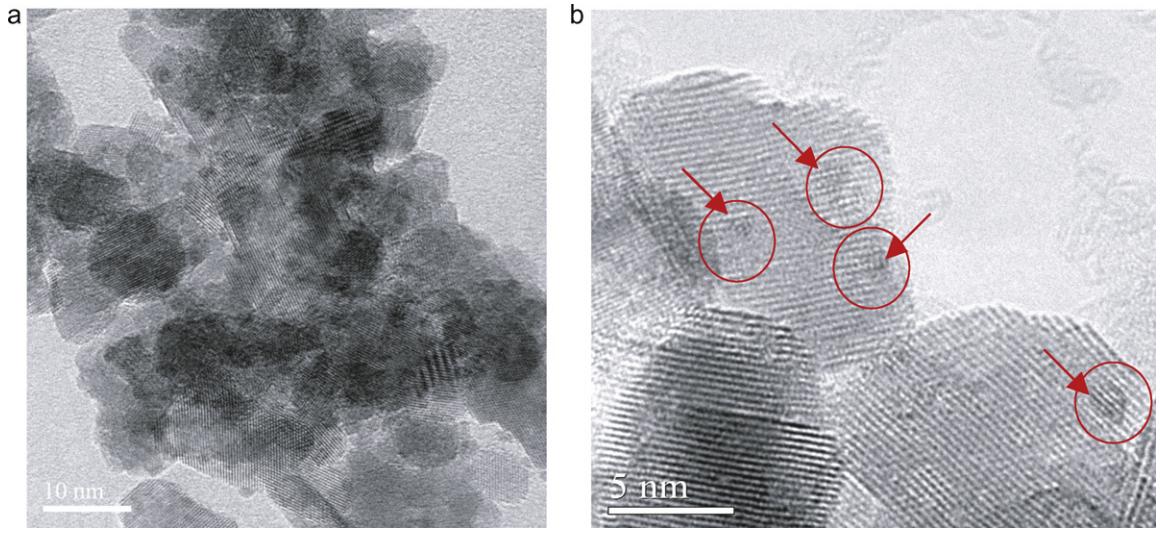

Fig. 6. TEM microphotographs (a and b) for the Pt/CeO_2-PD sample.

phenomena have been widely reported in the literature to occur, even at room temperature, in the case of noble metals supported on ceria [20,21].

On the basis of the above results it can be concluded that, under the experimental conditions used in this work, H_2 chemisorption is not an affordable technique to determine the Pt dispersion and average particle size of investigated Pt/TiO_2 and Pt/CeO_2 catalysts.

3.5. Catalytic activity measurements

Conversions of toluene and acetone as a function of the reaction temperature on supported Pt catalysts are reported in Fig. 8 (Pt/CeO_2 series) and Fig. 9 (Pt/TiO_2 series). It must be noted that on Pt/CeO_2 catalysts, analogously to that reported in the case of $Pt/\gamma\text{-}Al_2O_3$ [8], the oxidation reaction of both molecules proceeds directly to CO_2 with no significant formation of intermediate oxidation products. This also occurs on Pt/TiO_2 catalysts in acetone oxidation, whereas on titania samples small amounts of benzoic acid were also detected at low conversion in the case of toluene oxidation. It must also be underlined that on pure supports no reaction was observed up to 400 °C and 300 °C for toluene and acetone oxidation respectively. The figures show that on both investigated supports samples prepared by photo-deposition exhibit higher combustion activity for toluene or acetone than the corresponding samples prepared by impregnation. In particular on the Pt/CeO_2-PD sample the light off curve was significantly (100 °C or more) shifted to lower temperature with respect to the Pt/CeO_2-IM sample. A lower sensitivity to the preparation method was instead observed on the Pt/TiO_2 series, with the light off curve of the PD sample only 20 °C downshifted compared to the IM one. It is noteworthy that the catalytic activity of the Pt/CeO_2-PD sample is quite high, being comparable or even higher than that reported in the literature on highly active ceria-based catalysts, namely Al_2O_3–CeO_2 [22], Au/CeO_2 [13], Pt/CeO_2–ZrO_2 [23], $LaCoO_3$ loaded on $Ce_{1-x}Zr_xO_2$ [24].

4. Discussion

TEM data reported in the Results section clearly showed that the Pt catalysts prepared by the photo-deposition technique, both with ceria and titania as the support, exhibit small Pt nanoparti-

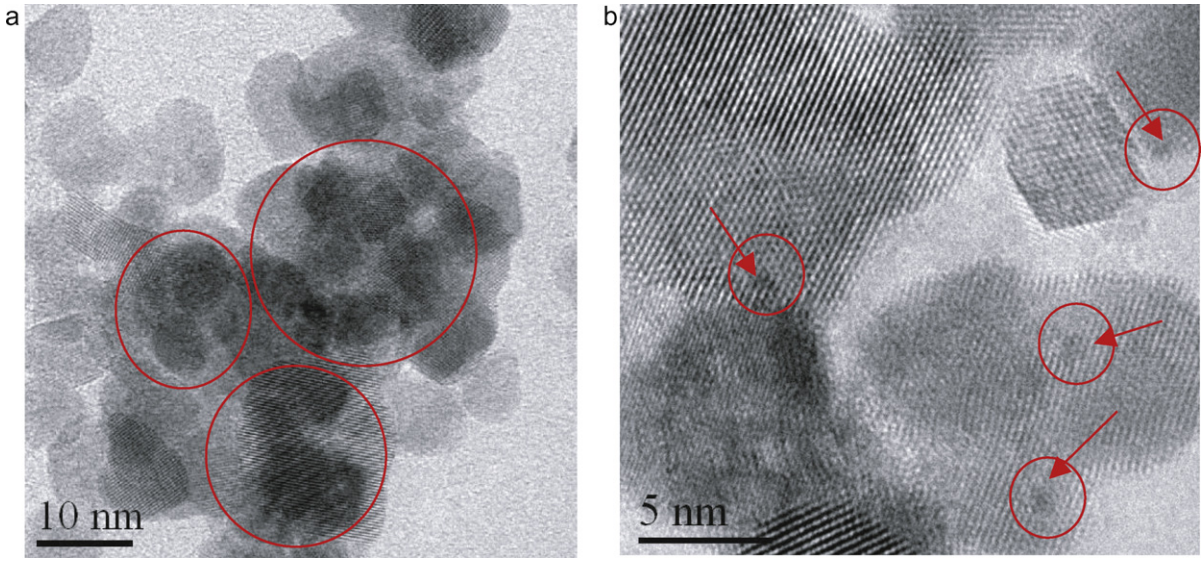

Fig. 7. TEM microphotographs (a and b) for the Pt/CeO_2-IM sample.

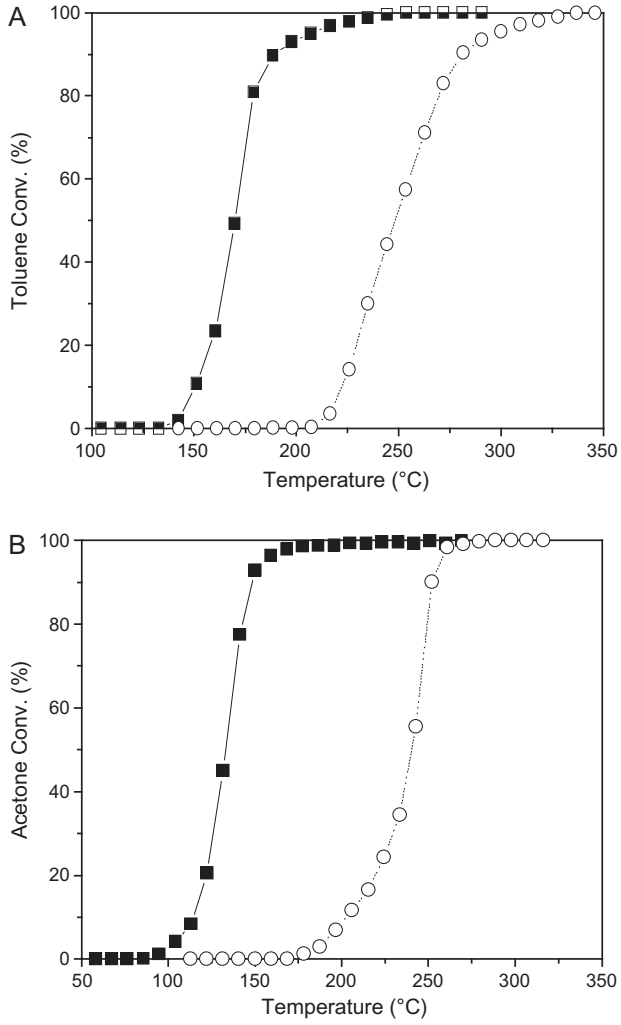

Fig. 8. Toluene (A) and acetone (B) oxidation over ceria supported Pt catalysts: (■, full line) PD samples; (○, dotted line) IM samples.

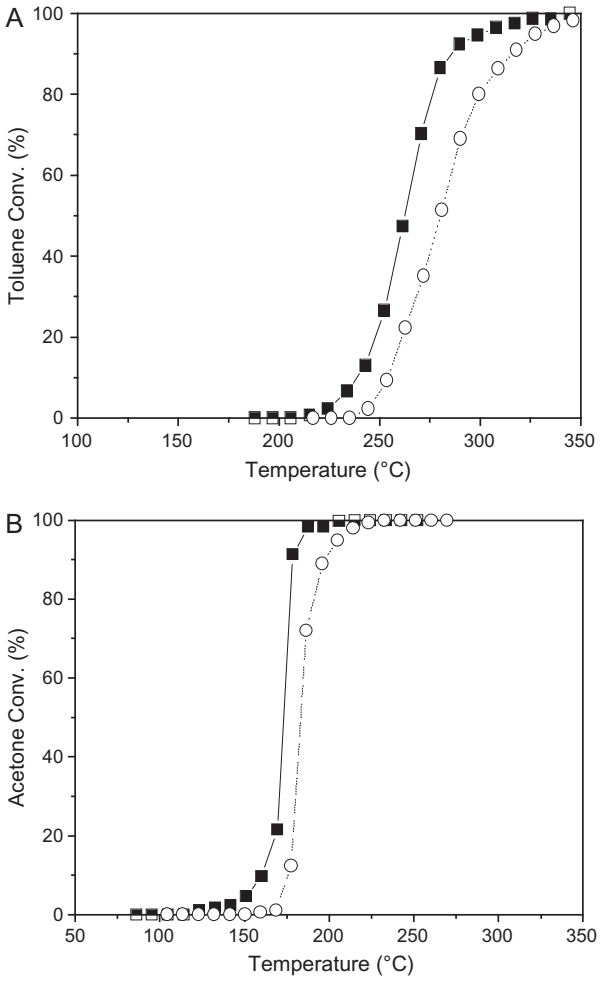

Fig. 9. Toluene (A) and acetone (B) oxidation over titania supported Pt catalysts: (■, full line) PD samples; (○, dotted line) IM samples.

cles with an average diameter of 1.6–2 nm. It is noteworthy that the size of Pt nanoparticles deposited on both supports was lower than that determined by DLS (5–6 nm) in the ethanol solution after photo-reduction in the absence of the support. It can be ruled out that this discrepancy is related to the different light intensities used in the kinetic (1×10^{-6} Nhν min^{-1}) and catalyst preparation experiments (1×10^{-5} Nhν min^{-1}), in so as with a light intensity of 1×10^{-5} Nhν min^{-1} we obtained the same DLS average size than that found using a lower light intensity (Supplementary data, Fig. 1). Moreover it is highly unlikely that, under the mild conditions of the deposition phase, the support can cause a disaggregation of metal nanoparticles resulting in smaller particles. It can be reasonably suggested that the TEM-DLS discrepancy can be rationalized considering that, whereas TEM determines the core diameter of the particle, DLS measures the hydrodynamic diameter in solution, including the ligand (Hacac) shell moving with the particle, and therefore can result in an overestimation of the particle size [25,26].

Another important feature of the Pt catalysts obtained by the LPPD approach is the high homogeneous spreading of Pt particles over the support surface with a monomodal and very narrow size distribution. This is in contrast with results of the catalysts prepared by the classical impregnation method which instead presented a quite heterogeneous distribution with evident massive aggregates of Pt units located around the edges of the support grains, together with very small particles. A similar behaviour has been previously reported on Pt/Al_2O_3 catalysts [8]. In fact a narrow monomodal particle size distribution centered at around 1.6 nm was found for Pt/Al_2O_3 samples prepared by LPPD whereas on the impregnated sample Pt nanoparticles were less uniformly distributed in size, exhibiting a bimodal distribution, with several Pt particles (60% ca. of the total number) smaller than 1.4 nm and some larger ones, with sizes ranging between 2.8 and 4 nm. It is important to underline that the different platinum morphology of PD and IM samples cannot be ascribed to the different pre-treatment conditions of these samples (the IM sample was prepared in H_2 atmosphere at 350 °C whereas the PD sample was obtained at room temperature). In fact, we verified that the PD sample treated under the same conditions as the IM one (H_2 atmosphere at 350 °C) exhibits the same structural features as well as catalytic performances (Supplementary data, Fig. 2) as the as-prepared PD catalyst. Therefore it can be concluded that the liquid phase photo-deposition represent a reliable technique for the preparation of highly dispersed supported Pt catalysts with an uniform distribution of the metal on the support, which is independent upon the nature of the support as well as the experimental procedure employed. In fact, the same distribution was obtained carrying out the photo-reduction in the presence of the support, i.e., nanoparticles formation and deposition steps taking place simultaneously, as reported in the case of Pt/Al_2O_3 samples [8], or adding the support to the solution after the platinum photo-reduction, i.e., performing nanoparticles formation and deposition in two separate steps, as shown on Pt/CeO_2 and Pt/TiO_2 catalysts in the present paper.

Before discussing catalytic activity results it is important to recall that there is a general agreement on the fact that over platinum and palladium catalysts supported on non reducible oxides (such as alumina) the deep oxidation of light alkanes, aromatic hydrocarbons and oxygenated compound is a structure sensitive reaction, involving the activation of the oxygen on the noble metal. However some conflicting results were reported in the literature on the extent of this effect as well as on which particle size of the active metal is the optimal one [27–32]. When reducible oxides (such as ceria and to a minor extent titania) are used as supports of noble metals, oxidation activity has been found to depend on both the oxygen activation on the active metal and the capacity of the oxide of providing active lattice oxygens, involved in the reaction through a Mars–Van Krevelen mechanism [12,33–35]. Therefore both the status of the metal and the properties of the oxide can play a key role in addressing the catalytic performance of these systems.

Catalytic results reported in this paper point out that the Pt/CeO_2 catalyst prepared through the photo-deposition approach exhibits much better performance in the VOC deep oxidation compared to the impregnated sample. In order to explain this behaviour it must be reminded that, as reported in the literature, the high activity of metal/ceria catalysts towards oxidation reactions has been attributed to the enhanced reactivity of CeO_2 surface oxygens induced by the metal, which causes a decrease in the strength of the surface Ce–O bonds adjacent to the active metal atoms thus leading to a higher surface lattice oxygen mobility of ceria [12,36,37]. On the basis of TEM data the higher activity of the sample prepared by the photochemical approach with respect to the impregnated one can be reasonably related to the presence on the PD sample of platinum nanoparticles with highly uniform diameter in the range 1.6–2 nm, which can be considered appropriate for VOC deep oxidation, providing a highly efficacious oxygen activation. On very small Pt particles, found to be numerous on the impregnated sample, where corners, edges and higher energy faces exposed predominate, adsorbed oxygen is bonded too tightly on the active metal surface thus resulting in a low reactivity towards the oxidation [8,27]. Moreover, it must be taken into account that the highly homogeneous spreading of Pt particles over the support, found for the PD catalyst, could be also claimed in order to explain the higher activity of this sample. In fact, in order to perform its positive function in enhancing the reactivity of CeO_2 surface oxygens, the metal particles must be in close contact with the support; therefore Pt particles more homogeneously distributed on the support surface should result in a much more efficacious interaction with lattice ceria oxygens. However, it cannot be ruled out that the lower activity of the impregnated samples can be also negatively affected by the presence of residual chlorine arising from the Pt precursor used to prepare Pt-IM catalysts [38,39].

Analogous to Pt/CeO_2 series, the Pt/TiO_2 sample prepared by photo-deposition resulted to be more active compared to the impregnated one, but in this case the difference in the activity between these two samples was considerably lower than observed on the ceria catalysts. The lower influence of the preparation method towards the oxidation of VOC can be reasonably ascribed to the lower oxygen mobility of the titania, so the extent of the effect of the different size and morphology of the Pt nanoparticles results to be much less powerful. Presumably, on titania supported catalysts the activation of oxygen on Pt sites plays a key role in affecting the catalytic properties of the system.

Interestingly, the comparison of catalytic results reported in Figs. 8 and 9 shows that the Pt/TiO_2-PD catalyst is much less active than the corresponding Pt/CeO_2-PD one, despite similar Pt particle size distributions were found on both samples. According to the reaction mechanism above discussed, this behaviour well agrees with the higher oxygen lattice mobility/reactivity of ceria compared to titania [21], pointing to the key role played by the support in addressing the catalytic properties of these systems. On the contrary the oxidation activity of both samples prepared by impregnation (Pt/TiO_2-IM and Pt/CeO_2-IM) is almost comparable. This behaviour can be rationalized considering that, on the impregnated sample, Pt nanoparticles were non homogeneously spread over the support surface, showing massive Pt aggregation phenomena. This should prevent platinum from an efficacious activation of the lattice oxygen of the support, thus minimizing the role of the oxide in the VOC deep oxidation.

5. Conclusions

On the basis of the obtained results it can be concluded that the photochemical approach here reported, consisting in the photoreduction at room temperature in ethanol of a soluble platinum complex and the subsequent deposition on a specific support, represents a reliable method for the preparation of supported platinum catalysts with an homogeneous and very narrow Pt size distribution, found to be substantially independent from the support used. Interestingly this distribution resulted to be appropriate for the deep oxidation of toluene and acetone. Further advantages of this technique appear to be the possibility to work at room temperature with simple and low cost equipments, which makes this synthetic approach interesting both from an economic and environmental point of view.

Appendix A. Supplementary data

Supplementary data associated with this article can be found, in the online version, at doi:10.1016/j.molcata.2010.10.003.

References

[1] G. Ertl, H. Knözinger, J. Weitkamp (Eds.), Preparation of Solid Catalysts, Wiley, Weinheim, 1999.
[2] B.C. Gates, Catalytic Chemistry, John Wiley and Sons, New York, 1992.
[3] O.S. Alexeev, B.C. Gates, Top. Catal. 10 (2000) 273–293.
[4] O.S. Alexeev, A. Siani, G. Lafaye, C.T. Williams, H.J. Ploehn, M.D. Amiridis, J. Phys. Chem. B 110 (2006) 24903–24914.
[5] A. Roucoux, J. Schulz, H. Patin, Chem. Rev. 102 (2002) 3757–3778.
[6] B.C. Gates, Chem. Rev. 95 (1995) 511–522.
[7] A. Siani, K.R. Wigal, O.S. Alexeev, M.D. Amiridis, J. Catal. 257 (2008) 16–22.
[8] C. Crisafulli, S. Scirè, S. Giuffrida, G. Ventimiglia, R. Lo Nigro, Appl. Catal. A: Gen. 306 (2006) 51–57.
[9] A. Peled, Lasers Eng. 6 (1997) 41–79.
[10] S. Giuffrida, L.L. Costanzo, G.G. Condorelli, G. Ventimiglia, I.L. Fragalà, Inorg. Chim. Acta 358 (2005) 1873–1881.
[11] S. Scirè, C. Crisafulli, S. Giuffrida, C. Mazza, P.M. Riccobene, A. Pistone, G. Ventimiglia, C. Bongiorno, C. Spinella, Appl. Catal. A: Gen. 367 (2009) 138–145.
[12] J.G. Eden, Chemical Analysis, vol. 122, Wiley, New York, 1992.
[13] S. Scirè, S. Minicò, C. Crisafulli, C. Satriano, A. Pistone, Appl. Catal. B: Environ. 40 (2003) 43–49.
[14] J. Calvert, J.N. Pitts, Experimental Methods in Photochemistry, John Wiley and Sons, New York, 1966, p. 783.
[15] H. Nakanishi, H. Morita, S. Nagakura, Bull. Chem. Soc. Jpn. 50 (1977) 2255–2261.
[16] J. Park, J. Joo, G.S. Kwon, Y. Jang, T. Hyeon, Angew. Chem. Int. Ed. 46 (2007) 4630–4660.
[17] M.B. Kasture, P. Patel, A.A. Prabhune, C.V. Ramana, A.A. Kulkarni, B.L.V. Prasad, J. Chem. Sci. 120 (2008) 515–520.
[18] S.J. Tauster, Acc. Chem. Res. 20 (1987) 389–394.
[19] M.-Y. Kim, Y. San You, H.-S. Han, G. Seo, Catal. Lett. 120 (2008) 40–47.
[20] A. Trovarelli, Catalysis by Ceria and Related Materials, Imperial College Press, London, 2002.
[21] S. Salasc, V. Perrichon, M. Primet, M. Chevrier, N. Mouaddib-Moral, J. Catal. 189 (2000) 401–409.
[22] G. Del Angel, J.M. Padilla, I. Cuauhtemoc, J. Navarrete, J. Mol. Catal. A: Chem. 281 (2008) 173–178.
[23] Z.M. Liu, J.L. Wang, J.B. Zhong, Y.Q. Chen, S.H. Yan, M.C. Gong, J. Hazard. Mater. 149 (2007) 742–746.
[24] M. Alifanti, M. Florea, V.I. Parvulescu, Appl. Catal. B: Environ. 70 (2007) 400–405.
[25] S.-J. Kim, S.-D. Oh, S.-H. Choi, A.I. Gopolan, K.-P. Lee, H.-D. Kang, C.-H. Shin, Korean J. Chem. Eng. 23 (2006) 488–495.
[26] K. Esumi, T. Matsumoto, Y. Seto, T. Yoshimura, J. Colloid Interface Sci. 284 (2005) 199–203.
[27] T.F. Garetto, C.R. Apesteguia, Catal. Today 62 (2000) 189–199.
[28] T.F. Garetto, C.R. Apesteguia, Appl. Catal. B: Environ. 32 (2001) 83–94.

[29] N. Radic, B. Grbic, A. Terlecki-Baricevic, Appl. Catal. B: Environ. 50 (2004) 153–159.
[30] C. Pliangos, I.V. Yentekakis, V.G. Papadakis, C.G. Vayenas, X.E. Verykios, Appl. Catal. B: Environ. 14 (1997) 161–173.
[31] P. Papaefthimiou, T. Ioannides, X.E. Verykios, Appl. Catal. B: Environ. 15 (1998) 75–92.
[32] P. Papaefthimiou, T. Ioannides, X.E. Verykios, Appl. Catal. B: Environ. 13 (1997) 175–184.
[33] S. Minicò, S. Scirè, C. Crisafulli, R. Maggiore, S. Galvagno, Appl. Catal. B: Environ. 28 (2000) 245–251.
[34] M. Baldi, E. Finocchio, F. Milella, G. Busca, Appl. Catal. B: Environ. 16 (1998) 43–51.
[35] E.M. Cordi, P.J. O'Neill, J.L. Falconer, Appl. Catal. B: Environ. 14 (1997) 23–36.
[36] Q. Fu, A. Weber, M. Flytzani-Stephanopoulos, Catal. Lett. 77 (2001) 87–95.
[37] C. Serre, F. Garin, G. Belot, G. Maire, J. Catal. 141 (1993) 1–8.
[38] N.W. Cant, D.E. Angove, M.J. Patterson, Catal. Today 44 (1998) 93–99.
[39] J. Silvestre-Albero, F. Coloma, A. Sepulveda-Escribano, F. Rodriguez-Reinoso, Appl. Catal. A: Gen. 304 (2006) 159–167.